INT. REVIEWS IN PHYSICAL CHEMISTRY, 2002
VOL. 21, NO. 2, 257–275

Phenomena of *g-u* symmetry-breakdown in HD

A. DE LANGE*, E. REINHOLD† and W. UBACHS‡
Laser Centre, Department of Physics and Astronomy, Vrije Universiteit, Amsterdam, The Netherlands

Phenomena associated with the breakdown of inversion symmetry in the HD molecule are reviewed and discussed. A distinction is made between three kinds of physical effects observed in HD spectra. The existence of a small electric dipole moment in the ground state gives rise to vibrational and pure rotational transitions following selection rules of electric dipole transitions. Coupling between electronic states of *g* and *u* symmetry occurs, which is associated with the appearance of forbidden lines in the electronic spectrum. This effect occurs predominantly at near coincidences between levels of opposite inversion symmetry and a recently observed example of strongly interacting states ($\bar{H}\,^1\Sigma_g^+$ and $\bar{B}\,^1\Sigma_u^+$) is highlighted. Electronic coupling between states of *g* and *u* symmetry always takes place near dissociation threshold; as a result of the mass difference and the electronic isotope shift the behaviour at long range cannot be described in an adiabatic picture. A procedure is developed to construct long-range potentials near the $n = 2$ dissociation limit in which the breakdown of *g*–*u* symmetry is incorporated.

Contents

1. Introduction

Symmetry is a basic concept in physics. Symmetry properties of physical laws impose restraints on the structure of matter and therefore, when characterizing a system, it is important to identify its symmetry properties. A diatomic molecule possesses symmetries of strict validity, for instance the permutation of identical particles, together with some symmetries of only approximate validity. One such

Email: * arno@nat.vu.nl
Email: † Elmar.Reinhold@lac.u-psud.fr
Email: ‡ wimu@nat.vu.nl

International Reviews in Physical Chemistry ISSN 0144–235X print/ISSN 1366–591X online © 2002 Taylor & Francis Ltd
http://www.tandf.co.uk/journals
DOI: 10.1080/01442350210124515

approximate symmetry is the inversion symmetry of the electronic wavefunction in homonuclear diatomic molecules. In these molecules, this symmetry is valid to a very high degree and electronic states are therefore often labelled with *gerade* or *ungerade*; these are the two eigenvalues of the inversion symmetry operator. Although the symmetry will be broken at a certain point in homonuclear molecules, it will be broken in heteronuclear isotopomers at a lower level. In HD, for instance, the breaking of this symmetry is observed in several ways.

A celebrated example of breaking of inversion symmetry in HD is the occurrence of an electric dipole moment, which had already been predicted by Wick [1] 1935. The centre of positive charge oscillates along the molecular axis during vibration, because the excursions of the proton are larger than those of the deuteron; since the electrons do not follow this motion exactly, a permanent dipole moment results. Herzberg was the first to observe the features of an infrared, i.e. vibrational, spectrum in HD, following the selection rules of an electric dipole transition [2], whereas Bunker investigated the transitions and in particular the line strengths, theoretically [3]. Later, the pure rotational spectrum in the far infrared domain, also associated with the ground-state dipole moment, was observed as well [4]. A collective shift of vibrational levels in the $X\,^1\Sigma_g^+$ ground state of HD with respect to the expected values based on the levels in H_2 and D_2 is observed. This effect is on the order of $0.5\,cm^{-1}$, which is attributed to non-adiabatic interactions with higher-lying states of $^1\Sigma_u^+$ symmetry [5], the interaction that is responsible for the electric dipole moment of the ground state.

The breakdown of the *g–u* symmetry is also observed *via* otherwise dipole forbidden $g \leftrightarrow g$ electronic transitions. This is for instance the case with the $EF\,^1\Sigma_g^+$–$X\,^1\Sigma_g^+$ system, first observed by Dabrowski and Herzberg [5] and later in higher resolution by Hinnen *et al.* [6]. The symmetry-breaking effect is strongest for those rovibrational levels that are close to levels of the B and C states, with $^1\Sigma_u^+$ and $^1\Pi_u$ symmetry, respectively. Similarly, forbidden electronic transitions were observed in the $GK\,^1\Sigma_g^+$–$X\,^1\Sigma_g^+$ and $I\,^1\Pi_g$–$X\,^1\Sigma_g^+$ systems [5]; in these cases rovibrational levels in the inner wells of the excited double-well structures could be probed. A similar, but stronger, feature of *g–u* symmetry breaking is that of the interacting $\bar{H}\,^1\Sigma_g^+$ and $\bar{B}\,^1\Sigma_u^+$ states. The potential curves corresponding to these states, nearly coincide over a large range of internuclear separations and the progression of the vibrational levels is such that the interaction reaches a maximum near $v = 14$, to the extent of almost complete mixture of a $^1\Sigma_g^+$ and a $^1\Sigma_u^+$ vibrational level [7]. The features of such accidental behaviour are reviewed in section 2.

The former of the two aforementioned cases is an example of a weak interaction as the perturbing states are localized in a different energy region to the electronic ground state. In the latter cases, the interactions are much stronger owing to coincidences. Near dissociation limits the density of bound states becomes high, because several potentials converge to the same limit. The spacing between levels within one potential decreases as the limit is approached and coincidences between rovibrational levels of different inversion symmetry will always occur. The interactions result in the splitting of the dissociation limit which is associated with the existence of an atomic isotope shift between H and D. A recent investigation of the $I'\,^1\Pi_g$ state [8], just below the $n = 2$ limit, revealed several aspects of the *g–u* symmetry breakdown close to a dissociation limit. A semiempirical treatment of this energetic region in HD is further elaborated in section 3. The potential curves belonging to the states discussed in this paper are depicted in figure 1.

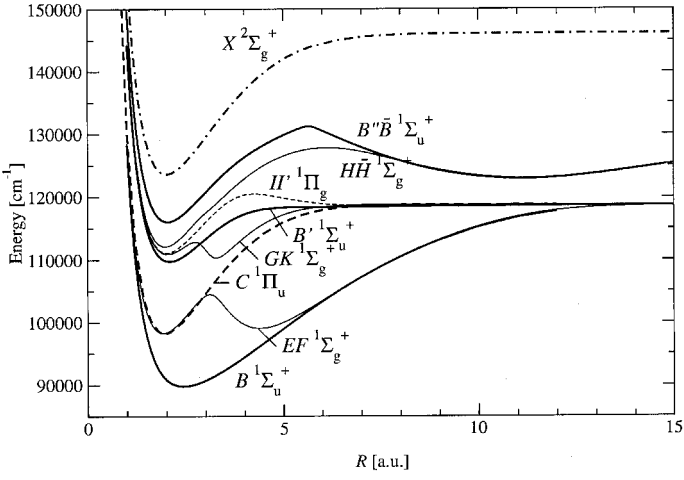

Figure 1. Potential curves for the $B\,^1\Sigma_u^+$, $B'\,^1\Sigma_u^+$, $C\,^1\Pi_u$, $EF\,^1\Sigma_g^+$, $GK\,^1\Sigma_g^+$, $II'\,^1\Pi_g$, $H\bar{H}\,^1\Sigma_g^+$ and $B''\bar{B}\,^1\Sigma_u^+$ states in hydrogen. The thick curves refer to *ungerade* states and the thin curves to *gerade* states. The Σ states are depicted with full curves; Π states with broken curves. The potential curve for the ground state of HD^+ is depicted as a dot-dashed curve.

To investigate to what level inversion symmetry holds in general, some aspects of the theory of molecular structure are discussed in the next subsection. The Born–Oppenheimer (BO) approximation [9], one of the so-called adiabatic approximations, decoupling the electronic wavefunction from the nuclear wavefunction, is taken as the starting point of the analysis.

1.1. *Adiabatic approximations*

The non-relativistic Schrödinger equation for diatomic molecules, after separating the centre-of-mass motion, can be written as (see for example [10, 11])

$$(H_0 + H_1 + H_2)\Psi(\boldsymbol{R}, \boldsymbol{r}) = E\Psi(\boldsymbol{R}, \boldsymbol{r}), \tag{1}$$

where

$$H_0 = -\frac{\hbar^2}{2m_e}\sum_i \nabla_{\boldsymbol{r}_i}^2 + V(R, \boldsymbol{r}),$$

$$H_1 = -\frac{\hbar^2}{2\mu}\nabla_{\boldsymbol{R}}^2, \quad \text{and}$$

$$H_2 = -\frac{\hbar^2}{2\mu_\alpha}\nabla_{\boldsymbol{R}} \cdot \sum_i \nabla_{\boldsymbol{r}_i} - \frac{\hbar^2}{8\mu}\sum_{i,j} \nabla_{\boldsymbol{r}_i} \cdot \nabla_{\boldsymbol{r}_j}, \tag{2}$$

with m_e the electron mass, $\mu = M_1M_2/(M_1 + M_2)$ the reduced mass of nuclei 1 and 2 and $\mu_\alpha = M_1M_2/(M_1 - M_2)$. $\boldsymbol{R}$ refers to the nuclear coordinates in a fixed reference system, $\boldsymbol{r}$ to coordinates of all electrons, whereas $\boldsymbol{r}_i$ refers to the coordinates of the ith electron only. $R = |\boldsymbol{R}|$ is the internuclear distance. H_0 represents the electronic Hamiltonian; the first term corresponds to the kinetic energy of the electrons and the second to the potential energy representing the Coulomb attraction and repulsion between all charged particles. H_1 is the kinetic energy term of the nuclei and H_2

represents the coupling of the electrons with the nuclei and the electron–electron coupling. Without imposing restraints on generality, one can express the wavefunction $\Psi(\boldsymbol{R},\boldsymbol{r})$ as the following expansion:

$$\Psi(\boldsymbol{R},\boldsymbol{r}) = \sum_n \chi_n(\boldsymbol{R})\phi_n(R,\boldsymbol{r}), \tag{3}$$

where $\phi_n(R,\boldsymbol{r}_i)$ is one of the complete set of orthonormal eigenstates of H_0 and n is the label for a particular eigenstate, thus

$$H_0\phi_n(R,\boldsymbol{r}) = E_n(R)\phi_n(R,\boldsymbol{r}). \tag{4}$$

In this equation the internuclear distance R is a parameter, rather than a variable and E_n is therefore a function of R.

Inserting the expansion of equation (3) in the Schrödinger equation, equation (1), subsequently multiplying by the complex conjugate of $\phi_m(R,\boldsymbol{r})$ and integrating over all the electronic coordinates results in [11]

$$\left[-\frac{\hbar^2}{2\mu}\nabla^2_{\boldsymbol{R}} + E_m(R) + C_{mm}(R)\right]\chi_m(\boldsymbol{R}) = E\chi_m(\boldsymbol{R}) - \sum_{n\neq m} C_{mn}\chi_n(\boldsymbol{R}), \tag{5}$$

where

$$C_{mn} = \int \phi^*_m(R,\boldsymbol{r})H_2\phi_n(R,\boldsymbol{r})\,\mathrm{d}\boldsymbol{r}. \tag{6}$$

To solve this infinite number of coupled equations self-consistently is virtually impossible and appropriate approximations are required.

In the BO approximation H_2 in equation (1) is ignored and hence all C_{mn} in equation (5) are set to zero. The equation reduces to

$$\left[-\frac{\hbar^2}{2\mu}\nabla^2_{\boldsymbol{R}} + E_m(R)\right]\chi_m(\boldsymbol{R}) = E^{\mathrm{BO}}\chi_m(\boldsymbol{R}), \tag{7}$$

with E^{BO} the energies within the BO approximation. The potential curves $E_m(R)$ are independent of the nuclear masses and are thus equal for all isotopomers within this approximation. The above equation provides a set of rovibrational $\chi_m(\boldsymbol{R})$ eigenfunctions for each potential curve $E_m(R)$ and the total molecular wavefunctions are simply of the form

$$\Psi(\boldsymbol{R},\boldsymbol{r}) = \phi(R,\boldsymbol{r})\chi(\boldsymbol{R}). \tag{8}$$

Approximations resulting in wavefunctions that can be written in such product forms are called adiabatic approximations. It can be shown that these approximations are valid only if the electronic wavefunction can be assumed to adapt instantaneously to the motion of the nuclei.

The BO approximation is an example of a rather crude, although often accurate, adiabatic approximation because a part of the Hamiltonian is completely neglected. One might wonder whether there is an adiabatic approximation which takes the neglected terms, at least partly, into account. It can be shown that only the second term in H_2 contributes to C_{mm} in equation (5) [11] and therefore C_{mm} is a function of R only. By ignoring the terms with C_{mn} $(m \neq n)$ in equation (5), a Schrödinger equation similar to the one in the BO approximation is obtained, namely

$$\left[-\frac{\hbar^2}{2\mu}\nabla_{\boldsymbol{R}}^2 + E'_m(R)\right]\chi_m(\boldsymbol{R}) = E^{\mathrm{ad}}\chi_m(\boldsymbol{R}), \tag{9}$$

where

$$E'_m(R) = E_m(R) + C_{mm}(R). \tag{10}$$

Also in this approximation the wavefunction belonging to the energy E^{ad} is simply a product of $\chi(\boldsymbol{R})$ and $\phi(R,\boldsymbol{r})$ and is therefore another example of an adiabatic approximation. C_{mm} can be viewed as corrections to the BO potentials and are consequently called the adiabatic corrections. The nuclear masses are contained in $C_{mm}(R)$ and this results in a different potential curve for every isotopomer. Note that when the nuclear masses are set to infinity, $C_{mm}(R) = 0$ and the BO curves are obtained again. Non-adiabatic corrections involve the matrix elements C_{mn} $(m \neq n)$ and result in wavefunctions which cannot be written as simple product functions. Therefore, $E'_m(R)$ are the 'best possible' potential energy curves.

1.2. *Inversion symmetry*

In diatomic molecules a symmetry operator i can be defined, which inverts the electronic part of the wavefunction through the geometrical centre of the molecule in the body-fixed frame. In homopolar diatomics, these being molecules consisting of two atoms with the same nuclear charge, the Coulomb field of the nuclei is invariant under this operation and hence the states can be divided in two classes: the eigenvalues $+1$ and -1 are represented by the labels g for *gerade* and u for *ungerade*, rather than '+' and '−' to avoid confusion with the eigenvalues of the parity operator acting in the space-fixed frame.

The first term of H_2 in equation (2), i.e.

$$H_{gu} = -\frac{\hbar^2}{2\mu_\alpha}\nabla_{\boldsymbol{R}} \cdot \sum_i \nabla_{\boldsymbol{r}_i}, \tag{11}$$

is the only term in the non-relativistic Hamiltonian not commuting with the operator i. The term represents the coupling between the electronic motion and the asymmetric rovibrational motion of the nuclei around the centre of mass, breaking the g–u symmetry.

As mentioned above, within the BO approximation, this term is neglected and g/u is a good quantum number. Also in the adiabatic approximation described by equation (9), g/u is a good quantum number as this term does not contribute to C_{mm} [11]. This extends to the case of isotopomers with nuclei of different mass like HD. In the case of homonuclear isotopomers $\mu_\alpha = 0$ and H_{gu} obviously vanishes completely and consequently the entire non-relativistic Hamiltonian commutes with i and g/u is a good quantum number even beyond adiabatic approximations. In heteronuclear isotopomers, however, it may reach considerable values and consequently may give rise to breakdown of the inversion symmetry. The breakdown of g–u symmetry in HD may be observed in different ways, but the origin lies predominantly in this coupling.

It is noted here that in the relativistic Hamiltonian another term does not obey symmetry under the i operation, namely the hyperfine interaction, involving the nuclear spin. This interaction breaks down the g–u symmetry in any isotopomer but is rather weak; $< 0.1\,\mathrm{cm}^{-1}$ at the $n = 2$ dissociation limit in H_2.

2. Forbidden electronic transitions

In the energy region in between $100\,000\,\mathrm{cm}^{-1}$ above the ground state and the $n = 2$ dissociation limit the rovibrational levels in the EF $^1\Sigma_g^+$ state of g symmetry and the B $^1\Sigma_u^+$ and C $^1\Pi_u$ states of u symmetry have several near coincidences, in HD as well as in homonuclear species. The transition EF $^1\Sigma_g^+$–X $^1\Sigma_g^+$ is dipole forbidden owing to the dipole selection rule $g \not\leftrightarrow g$. In HD, however, g is no longer a good quantum number and this selection rule becomes less strict. As a result of interactions the EF–X transitions in HD gain strength from interactions with the u symmetry states. Dabrowski and Herzberg [5] have observed various dipole-forbidden transitions originating in EF ($v = 2$–23) in absorption. They also have observed some other $g \leftrightarrow g$ transitions: G $^1\Sigma_g^+$–X $^1\Sigma_g^+$ and I $^1\Pi_g$–X $^1\Sigma_g^+$. Of the G state $v = 0$–3 was observed whereas $v = 0$ and $v = 3$ of the I state were identified. Later Hinnen *et al.* [6] performed a high-precision $1 + 1$ resonance enhanced multi-photon ionization experiment and observed EF $^1\Sigma_g^+$ ($v = 5$–8, 10–14). It was shown that the strongest transitions observed involved levels lying in energy in the vicinity of B and C states and therefore undergo the strongest interactions.

As a result of the interactions shifts in the level energies also occur. Hinnen *et al.* [6] analysed these shifts in terms of a semiempirical model of homogeneous and heterogeneous interactions between the three states involved. To treat the perturbations an energy matrix was diagonalized:

$$\begin{bmatrix} E_v^{\mathrm{B}}(J) & W_{\mathrm{B,C}}\tilde{J} & W_{\mathrm{B,EF}} \\ W_{\mathrm{B,C}}\tilde{J} & E_v^{\mathrm{C}}(J) & W_{\mathrm{C,EF}}\tilde{J} \\ W_{\mathrm{B,EF}} & W_{\mathrm{C,EF}}\tilde{J} & E_v^{\mathrm{EF}}(J) \end{bmatrix}, \tag{12}$$

where $\tilde{J} = \sqrt{J(J+1)}$ and the deperturbed eigenenergies are on the diagonal. The non-adiabatic interactions between the B $^1\Sigma_u^+$ and C $^1\Pi_u$ states, represented by a heterogeneous coupling (J-dependent matrix element), also occur in H_2 and D_2. The off-diagonal interactions $W_{\mathrm{C,EF}}\sqrt{J(J+1)}$ and $W_{\mathrm{B,EF}}$, representing g–u symmetry breaking, only play a role in HD. In the case of the strong interaction between B ($v = 14$) and EF ($v = 8$), with the closest coincidence appearing at $J = 3$, the interaction matrix element was found to be as large as $6.6\,\mathrm{cm}^{-1}$. A level diagram displaying the local g–u symmetry-breaking interactions between EF states of g symmetry and B and C states of u symmetry is shown in figure 2.

In the example of the $\bar{\mathbf{H}}\,^1\Sigma_g^+$ state, interacting with the $\bar{\mathbf{B}}\,^1\Sigma_u^+$ state, the g–u interactions are less accidental, because of the similar shapes of the two potential energy curves involved. As can be seen in figure 3 the vibrational spacing is slightly smaller in the $\bar{\mathbf{B}}\,^1\Sigma_u^+$ state then in the $\bar{\mathbf{H}}\,^1\Sigma_g^+$ outer-well state. Together with the fact that the lowest vibrational level of the $\bar{\mathbf{B}}$ state lies lower in energy than $v = 0$ of $\bar{\mathbf{H}}$, the interaction becomes stronger with increasing energy up to $v = 14$ where the two vibrational progressions cross each other. The avoided crossing behaviour in terms of frequency shifts and derived g/u mixing fractions are displayed in figure 4.

Experimentally both states were excited, in a multi-photon laser set-up, *via* the B $^1\Sigma_u^+$ intermediate state, although excitation of the $\bar{\mathbf{B}}$–B transition is dipole forbidden, because of the $u \not\leftrightarrow u$ selection rule; transition strength is gained from the interaction of the $\bar{\mathbf{B}}$ state with states of g symmetry, in particular $\bar{\mathbf{H}}$ and from B levels with an (accidentally) strong admixture of EF. In a semiempirical analysis, based on a comparison with the level energies for H_2 and D_2 in the $\bar{\mathbf{H}}$ state, the shifts were included in a perturbation analysis [7]; here only interactions with $\Delta v = 0$ were

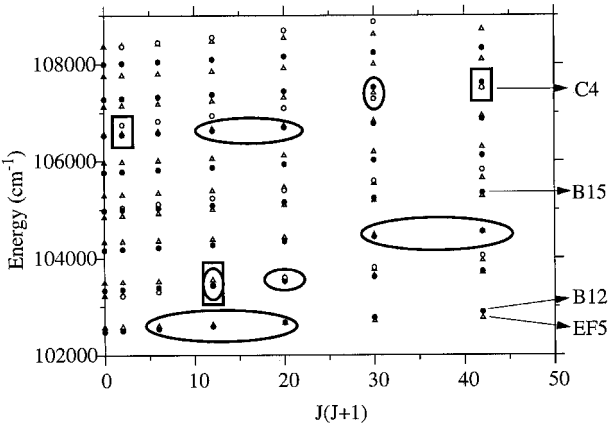

Figure 2. Energy level diagram (taken from [6]) displaying local perturbations between states of u and g symmetry in HD. Rotational quantum states in $B\,^1\Sigma_u^+$ are indicated by •, states of $C\,^1\Pi_u$ by ○ and states of $EF\,^1\Sigma_g^+$ by △. Local perturbations are indicated by rectangular or elliptical shapes: rectangular shapes refer to heterogeneous interactions between B and C levels; elliptical features involve g–u symmetry-breaking couplings between EF states and B and C states.

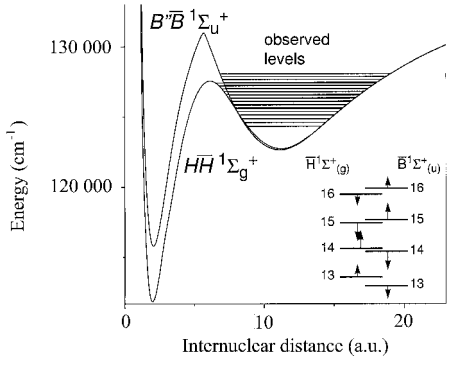

Figure 3. BO potential curves of the $H\bar{H}\,^1\Sigma^+_{(g)}$ and $B''\bar{B}\,^1\Sigma^+_{(u)}$ states taken from [12] and [13] respectively. Vibrational spacings in the $\bar{\mathbf{B}}$ outer well are larger than those in $\bar{\mathbf{H}}$, giving rise to a crossing near $v = 14$. In the inset it is shown how the levels are shifted around $v = 14$.

taken into account and the matrix element $\langle \bar{\mathbf{H}}(v)|H_{gu}|\bar{\mathbf{B}}(v)\rangle$ was found to be independent of the vibrational quantum number. Even in this restricted semiempirical model good quantitative agreement could be produced. The increase of interaction strength toward $v = 14$ is not produced by a variation of the matrix element but by the fact that the levels $\bar{\mathbf{B}}(v)$ and $\bar{\mathbf{H}}(v)$ approach each other. As shown in figure 4, for vibrational levels $v \neq 14$ there is a gradually increasing symmetry-breaking effect toward the crossing; at $v = 14$ there is nearly a 50%–50% admixture of g and u character in the $\bar{\mathbf{H}}\,^1\Sigma^+_{(g)}$ and $\bar{\mathbf{B}}\,^1\Sigma^+_{(u)}$ wavefunctions, where g and u have entirely lost meaning.

Above the potential barrier of $\bar{\mathbf{H}}$, the rovibronic wavefunctions extend to short internuclear distances and levels strongly interact with the short-lived Rydberg states. Therefore, the levels of the $\bar{\mathbf{H}}$ state become broadened. In HD the levels of the $\bar{\mathbf{B}}$ state are broadened as well, even though the levels are still beneath the barrier

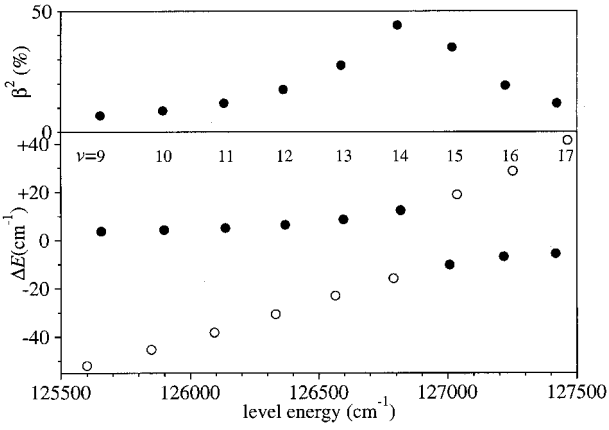

Figure 4. Perturbation analysis of the g–u mixing near $v = 14$ in both $H\bar{H}\,^1\Sigma^+_{(g)}$ and $B''\bar{B}\,^1\Sigma^+_{(u)}$ states. A typical anticrossing pattern results in the lower panel. ΔE = (observed level energy) – (energy of unperturbed $\bar{H}$ level). At $v = 14$ the largest mixing between the *gerade* and *ungerade* states is to be expected and indeed, as can be seen in the upper panel, the mixing is almost 50%–50%.

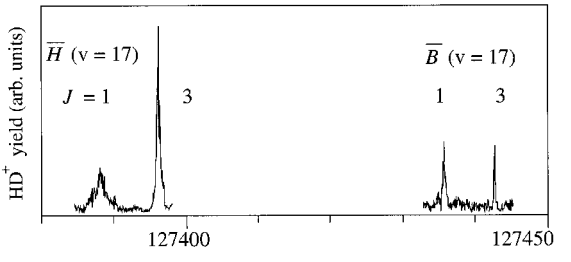

Figure 5. Observed spectra of $B''\bar{B}\,^1\Sigma^+_{(u)}$ $(v = 17)$ and $H\bar{H}\,^1\Sigma^+_{(g)}$ $(v = 17)$ levels in excitation from the $B\,^1\Sigma^+_u$ $(v = 21, J = 2)$ intermediate state. The energy of the $\bar{H}$ $(v = 17,$ $J = 1, 3)$ levels is well above the barrier in $H\bar{H}$ and it is bound by the u character in the wavefunction.

of the $\bar{B}$ potential. In the case of H_2 these levels are shielded by this barrier from the predissociating and autoionizing Rydberg states. In HD, however, the levels couple with levels in the $\bar{H}$ state and interact *via* this admixture with the Rydberg levels and become shorter lived than the same levels in H_2. This phenomenon is demonstrated in the recording of $v = 17$ levels for both $\bar{H}$ and $\bar{B}$ in figure 5. The $\bar{H}$ $(v = 17)$ level is well above the barrier of the g symmetry potential and couples therefore to the continuum states at short internuclear separation for which strong broadening is predicted and it can be seen that the linewidths are of the order of wavenumbers. Also the $\bar{B}$ $(v = 17)$ level is slightly broadened, not to the extent of the $\bar{H}$ counterpart, but broader than comparable levels in H_2. Because of the interaction with the $\bar{H}$ $(v = 17)$ state, the rotational levels become short-lived and hence the resonance becomes broad. Another peculiar effect can be seen in figure 5; the line corresponding to $\bar{H}$ $(v = 17, J = 3)$ is much narrower than the one belonging to $J = 1$. This may be explained in terms of coupling with the short-lived states at small internuclear distances. Probably, the $J = 3$ state undergoes a weaker interaction with the Rydberg manifold than the $J = 1$ state. This is supported by the fact that the lines corresponding to $\bar{B}$ $(v = 17)$ show the same behaviour.

Most of the features of this *g–u* symmetry-breaking phenomenon can be understood semiempirically and from a perturbation analysis only invoking $\Delta v = 0$ matrix elements in the coupling between $\bar{\mathbf{H}}$ and $\bar{\mathbf{B}}$ states. However, for the interaction between $\bar{\mathbf{H}}$ and $\bar{\mathbf{B}}$, accurate *ab initio* calculations were performed on the relativistic potentials of both electronic states and on the non-adiabatic matrix elements originating from equation (11). In these calculations the effects of all interacting vibrational levels are included, i.e. also $\Delta v \neq 0$. From a detailed comparison between experimentally determined level energies above the $X\,^1\Sigma_g^+$ $(v = 0, J = 0)$ ground state and calculation, agreement to within $1.5\,\mathrm{cm}^{-1}$ is found [13]. Only at excitation energies where tunnelling through the potential barrier becomes a dominant effect do the discrepancies grow. This is due to the neglect in the calculations of the interaction with Rydberg states at short internuclear separation.

3. Asymptotic behaviour of electronic states near the $n = 2$ limit in HD

We will show that, in HD, states at the dissociation threshold cannot, not even as an approximation, be described in the basis of g/u states. This means that BO potentials and actually all adiabatic potentials, cannot be used to describe the states at threshold. Moreover, it will be shown that, in heteronuclear isotopomers, the only possible long-range R dependence is R^{-6}. This in contrast to the homonuclear counterparts, where an R^{-3} asymptotic behaviour is found for the potential energy in some electronic states. This phenomenon of change of asymptotic behaviour is connected to the difference in mass of the nuclei. To account for the breakdown of the *g–u* symmetry, we first consider the possible potential energy curves representing the electronic states that correlate with one atom in $n = 1$ and one in $n = 2$. *A priori* it should be realized that, in view of the atomic isotope shift, there is not a single $n = 2$ dissociation limit. In HD there are two groups of limits, $\mathrm{H}(2\ell) + \mathrm{D}(1\mathrm{s})$ and $\mathrm{H}(1\mathrm{s}) + \mathrm{D}(2\ell)$, the latter $22.38\,\mathrm{cm}^{-1}$ higher in energy than the first and the adiabatic representation will therefore break down at threshold. In fact spin–orbit and hyperfine interactions give rise to further splittings, which will not be treated here since these effects are small ($< 0.2\,\mathrm{cm}^{-1}$) in HD.

The starting point is to express all the states converging to the $n = 2$ limit in terms of a sum over products of the one-electron wavefunctions of the atomic states. At the $n = 2$ limit one atom is in the 1s ground state and the other atom in either a 2s or a 2p state. The latter can be subdivided in a σ or a π orientation, with respect to the internuclear axis. In total there are two electrons, two nuclei and three different states, which adds up to 12 different permutations:

$$\begin{aligned}\Phi = {} & c_{111}\,\phi_{\mathrm{H}_{1\mathrm{s}}}(1)\phi_{\mathrm{D}_{2\mathrm{s}\sigma}}(2) + c_{121}\,\phi_{\mathrm{H}_{1\mathrm{s}}}(2)\phi_{\mathrm{D}_{2\mathrm{s}\sigma}}(1) \\ & + c_{211}\,\phi_{\mathrm{D}_{1\mathrm{s}}}(1)\phi_{\mathrm{H}_{2\mathrm{s}\sigma}}(2) + c_{221}\,\phi_{\mathrm{D}_{1\mathrm{s}}}(2)\phi_{\mathrm{H}_{2\mathrm{s}\sigma}}(1) \\ & + c_{112}\,\phi_{\mathrm{H}_{1\mathrm{s}}}(1)\phi_{\mathrm{D}_{2\mathrm{p}\sigma}}(2) + c_{122}\,\phi_{\mathrm{H}_{1\mathrm{s}}}(2)\phi_{\mathrm{D}_{2\mathrm{p}\sigma}}(1) \\ & + c_{212}\,\phi_{\mathrm{D}_{1\mathrm{s}}}(1)\phi_{\mathrm{H}_{2\mathrm{p}\sigma}}(2) + c_{222}\,\phi_{\mathrm{D}_{1\mathrm{s}}}(2)\phi_{\mathrm{H}_{2\mathrm{p}\sigma}}(1) \\ & + c_{113}\,\phi_{\mathrm{H}_{1\mathrm{s}}}(1)\phi_{\mathrm{D}_{2\mathrm{p}\pi}}(2) + c_{123}\,\phi_{\mathrm{H}_{1\mathrm{s}}}(2)\phi_{\mathrm{D}_{2\mathrm{p}\pi}}(1) \\ & + c_{213}\,\phi_{\mathrm{D}_{1\mathrm{s}}}(1)\phi_{\mathrm{H}_{2\mathrm{p}\pi}}(2) + c_{223}\,\phi_{\mathrm{D}_{1\mathrm{s}}}(2)\phi_{\mathrm{H}_{2\mathrm{p}\pi}}(1). \end{aligned} \tag{13}$$

The numerals in parentheses indicate which electron is attached to the nucleus indicated by the subscript. The atomic state is given in the subscript of ϕ. The coefficient c_{ijk} carries three indices, i to indicate which atom is in the ground state ($1 = \mathrm{H}$ and $2 = \mathrm{D}$), j being the electron attached to the ground state atom and k representing the state of the excited atom ($1 = 2s\sigma$, $2 = 2p\sigma$ and $3 = 2p\pi$). In equation (13) only the spatial part of the electronic wavefunction is considered.

The coefficients c_{ijk} are interconnected via symmetry properties. Under exchange of the electrons, the total wavefunction must be anti-symmetric. In the case of singlet states, the spin wavefunction is antisymmetric under the exchange of both electrons and the spatial part has to be symmetric. This means that $c_{11x} = c_{12x}$ and $c_{21x} = c_{22x}$ for singlet states and similarly for triplet states $c_{11x} = -c_{12x}$ and $c_{21x} = -c_{22x}$, in which x is 1, 2 or 3 (we neglect spin–orbit interaction). When the electronic part of the wavefunction is inverted with respect to the geometrical centre of the molecule, the excitation actually swaps from one atom to the other. The *gerade* states are by definition invariant under this operation and $c_{11x} = c_{21x}$ and $c_{12x} = c_{22x}$. In the case of *ungerade* states the relations are $c_{11x} = -c_{21x}$ and $c_{12x} = -c_{22x}$. This results in the following scheme:

$$\begin{aligned}
&c_{11x} = c_{12x} = c_{21x} = c_{22x} && {}^1\Lambda_g \\
&c_{11x} = c_{12x} = -c_{21x} = -c_{22x} && {}^1\Lambda_u \\
&c_{11x} = -c_{12x} = c_{21x} = -c_{22x} && {}^3\Lambda_g \\
&c_{11x} = -c_{12x} = -c_{21x} = c_{22x} && {}^3\Lambda_u. \qquad (14)
\end{aligned}$$

Twelve different potentials converge to the $n = 2$ dissociation limit. These can be subdivided in three groups of four potentials, each correlating with one of the three $1s + 2\ell\lambda$ limits. Four electronic states (${}^1\Sigma_g^+$, ${}^1\Sigma_u^+$, ${}^3\Sigma_g^+$ and ${}^3\Sigma_u^+$) correlate with $1s + 2s\sigma$. Another four Σ states (again ${}^1\Sigma_g^+$, ${}^1\Sigma_u^+$, ${}^3\Sigma_g^+$ and ${}^3\Sigma_u^+$) correlate with $1s + 2p\sigma$. Finally, four Π states (${}^1\Pi_g$, ${}^1\Pi_u$, ${}^3\Pi_g$ and ${}^3\Pi_u$), correlate with $1s + 2p\pi$. For every potential only the four coefficients described by equations (14) with the proper value for x are non-zero; all the other coefficients are equal to zero. This yields spatial wavefunctions for the electronic states, for which we give two examples:

$$\begin{aligned}
(1s2s)\,{}^1\Sigma_g^+ :\ & \phi_{\mathrm{H}_{1s}}(1)\phi_{\mathrm{D}_{2s\sigma}}(2) + \phi_{\mathrm{H}_{1s}}(2)\phi_{\mathrm{D}_{2s\sigma}}(1) \\
& + \phi_{\mathrm{D}_{1s}}(1)\phi_{\mathrm{H}_{2s\sigma}}(2) + \phi_{\mathrm{D}_{1s}}(2)\phi_{\mathrm{H}_{2s\sigma}}(1); \\
(1s2p)\,{}^3\Pi_u :\ & \phi_{\mathrm{H}_{1s}}(1)\phi_{\mathrm{D}_{2p\pi}}(2) - \phi_{\mathrm{H}_{1s}}(2)\phi_{\mathrm{D}_{2p\pi}}(1) \\
& - \phi_{\mathrm{D}_{1s}}(1)\phi_{\mathrm{H}_{2p\pi}}(2) + \phi_{\mathrm{D}_{1s}}(2)\phi_{\mathrm{H}_{2p\pi}}(1). \qquad (15)
\end{aligned}$$

These spatial wavefunctions must be multiplied by the appropriate spin wavefunctions to obtain the total electronic wavefunctions. This approach of constructing wavefunctions is only valid in homonuclear molecules, since we have imposed g or u symmetry.

Because of the isotope shift in atomic H and D the level energy for H($n\ell$) differs from D($n\ell$). This means that at a dissociation limit either one or the other atom is excited. Therefore, there is an alternative restriction in HD; if the two atoms are largely separated from each other, the excitation becomes localized, that is the

excitation is at either one of the atoms. If the H atom is excited (indicated by H^*) then $c_{11x} = c_{12x} = 0$ and if the D atom is excited (indicated by D^*) then $c_{21x} = c_{22x} = 0$ and equations (14) become

$$\begin{aligned}
&c_{11x} = c_{12x} = 0; c_{21x} = c_{22x} && {}^1\Lambda\,(H^*)\\
&c_{11x} = c_{12x}; c_{21x} = c_{22x} = 0 && {}^1\Lambda\,(D^*)\\
&c_{11x} = c_{12x} = 0; c_{21x} = -c_{22x} && {}^3\Lambda\,(H^*)\\
&c_{11x} = -c_{12x}; c_{21x} = c_{22x} = 0 && {}^3\Lambda\,(D^*).
\end{aligned} \tag{16}$$

These relations can be fulfilled only if each *g–u* couple of the same multiplet, converging to one of the limits, is completely mixed. The spatial wavefunctions at long range can be evaluated on substitution of the restraints on the coefficients as given in equation (16), yielding

$$\begin{aligned}
D(2s)^1\Sigma^+ &: \phi_{D_{1s}}(1)\phi_{H_{2s\sigma}}(2) + \phi_{D_{1s}}(2)\phi_{H_{2s\sigma}}(1)\\
H(2s)^1\Sigma^+ &: \phi_{H_{1s}}(1)\phi_{D_{2s\sigma}}(2) + \phi_{H_{1s}}(2)\phi_{D_{2s\sigma}}(1)\\
D(2p)^1\Sigma^+ &: \phi_{D_{1s}}(1)\phi_{H_{2p\sigma}}(2) + \phi_{D_{1s}}(2)\phi_{H_{2p\sigma}}(1)\\
H(2p)^1\Sigma^+ &: \phi_{H_{1s}}(1)\phi_{D_{2p\sigma}}(2) + \phi_{H_{1s}}(2)\phi_{D_{2p\sigma}}(1)\\
D(2p)^1\Pi &: \phi_{D_{1s}}(1)\phi_{H_{2p\pi}}(2) + \phi_{D_{1s}}(2)\phi_{H_{2p\pi}}(1)\\
H(2p)^1\Pi &: \phi_{H_{1s}}(1)\phi_{D_{2p\pi}}(2) + \phi_{H_{1s}}(2)\phi_{D_{2p\pi}}(1)\\
D(2s)^3\Sigma^+ &: -\phi_{D_{1s}}(1)\phi_{H_{2s\sigma}}(2) + \phi_{D_{1s}}(2)\phi_{H_{2s\sigma}}(1)\\
H(2s)^3\Sigma^+ &: -\phi_{H_{1s}}(1)\phi_{D_{2s\sigma}}(2) + \phi_{H_{1s}}(2)\phi_{D_{2s\sigma}}(1)\\
D(2p)^3\Sigma^+ &: -\phi_{D_{1s}}(1)\phi_{H_{2p\sigma}}(2) + \phi_{D_{1s}}(2)\phi_{H_{2p\sigma}}(1)\\
H(2p)^3\Sigma^+ &: -\phi_{H_{1s}}(1)\phi_{D_{2p\sigma}}(2) + \phi_{H_{1s}}(2)\phi_{D_{2p\sigma}}(1)\\
D(2p)^3\Pi &: -\phi_{D_{1s}}(1)\phi_{H_{2p\pi}}(2) + \phi_{D_{1s}}(2)\phi_{H_{2p\pi}}(1)\\
H(2p)^3\Pi &: -\phi_{H_{1s}}(1)\phi_{D_{2p\pi}}(2) + \phi_{H_{1s}}(2)\phi_{D_{2p\pi}}(1).
\end{aligned} \tag{17}$$

Thus, in the case of a heteronuclear molecule the g/u labels lose their meaning at the dissociation limit and the relations given in equations (14) are invalid.

The spin–orbit interaction is neglected and the spin is therefore a good quantum number. As a result the singlet potential curves and the triplet curves may be evaluated independently. Further, because of the cylindrical symmetry, Λ is also a good quantum number and the states of Σ and Π symmetry can also be treated separately. So, the four Π states can be evaluated in pairs and it has been shown that this gives good results [8]. To construct Σ potential curves in which the breakdown of the inversion symmetry is incorporated, the curves are also evaluated in pairs. This is not strictly valid; within each multiplet, four Σ potentials converge to the $n = 2$ limits

(see Table 17), two correlating with 2sσ and two with 2pσ. There are, however, some limitations in the way the four potentials may couple.

First, H_{gu} couples only states of different inversion symmetry. This can be seen as follows. H_{gu} is odd under inversion of the electronic coordinates:

$$iH_{gu} = -H_{gu}, \tag{18}$$

with i the inversion operator. Further,

$$\langle \phi_m | H_{gu} | \phi_n \rangle = 0, \tag{19}$$

if the integrand is an odd function and hence $\phi_m H_{gu} \phi_n$ must be an even function:

$$\begin{aligned} i(\phi_m H_{gu} \phi_n) &= (i\phi_m)(iH_{gu})(i\phi_n) \\ &= -(i\phi_m) H_{gu} (i\phi_n) \\ &= +(\phi_m H_{gu} \phi_n), \end{aligned} \tag{20}$$

which can only be satisfied if either ϕ_m is even and ϕ_n is odd or the other way around. Hence, two interacting states under the H_{gu} operator must be of different inversion symmetries. Thus, one potential couples at most with the two potentials of the other symmetry. If a $2s\sigma_{u(g)}$ state couples solely with a $2p\sigma_{g(u)}$ state, it can be shown that this would result in an unphysical long-range behaviour. Therefore, it is assumed that the interactions between $2s\sigma_g$ and $2s\sigma_u$ and between $2p\sigma_g$ and $2p\sigma_u$ are stronger than the interactions between states with different ℓ. In conclusion, as a first-order approximation, the Σ states will also be evaluated pairwise. Of course, very close to threshold, within the range of spin–orbit interaction, more states have to be evaluated at once. It is noted here that similar considerations will apply to the case of fine and hyperfine interactions as well.

Now we proceed with the construction of new potential energy curves, taking into account g–u symmetry breaking, for which the following eigenvalue problem has to be solved:

$$\begin{bmatrix} V_g(R) & H \\ H & V_u(R) \end{bmatrix} \Psi(R) = E(R)\Psi(R). \tag{21}$$

The two potentials V_g and V_u are the *gerade* and *ungerade* adiabatic potential curves of the same multiplicity converging to the same limit. H represents the interaction between the two states and is in principle a function of the internuclear distance R. As a first-order approximation, the value at $R = \infty$ can be used and equals half the energy-difference of the levels H(2ℓ) + D(1s) and H(1s) + D(2ℓ). This value (11.19 cm^{-1}) is determined using the value of the hydrogen–deuterium isotope shift of the 1S–2S transition as given in [14] with neglect of the fine structure; this splitting is the same for both isotopes up to an accuracy of 0.001 cm^{-1}. After diagonalization of the matrix of equation (21) two potentials are found, of which one converges to the H + D* limit and one to H* + D:

$$V_{\pm} = \frac{V_g + V_u}{2} \pm \sqrt{\left(\frac{V_g - V_u}{2}\right)^2 + H^2}, \tag{22}$$

where the + (−) sign refers to the upper (lower) dissociation threshold. The long-range interaction between two H atoms is governed by an attractive R^{-6} term in the case of the Σ states correlating with 1s + 2s. The states correlating with 1s + 2p are

dominated by an R^{-3} term. When the terms up to R^{-6} of the long-range potentials are substituted in equation (22), the following equations are obtained:

$$V_{\pm} = \frac{C_6^g + C_6^u}{2R^6} \pm \sqrt{\left(\frac{C_6^g - C_6^u}{2R^6}\right)^2 + H^2}, \tag{23}$$

for the potentials correlating with 1s + 2s and

$$V_{\pm} = \frac{C_3^g + C_3^u}{2R^3} + \frac{C_6^g + C_6^u}{2R^6} \pm \sqrt{\left(\frac{C_3^g - C_3^u}{2R^3} + \frac{C_6^g - C_6^u}{2R^6}\right)^2 + H^2}, \tag{24}$$

for the potentials correlating with 1s + 2p, where C_n^g and C_n^u are the coefficients of the nth term of the multipole expansion for the *gerade* and *ungerade* states respectively. For the latter case, $C_3^g = -C_3^u$ and $C_6^g = C_6^u$ [15] and hence equation (24) can be rewritten

$$V_{\pm} = \frac{C_6^g}{R^6} \pm \sqrt{\left(\frac{C_3^g}{R^3}\right)^2 + H^2}. \tag{25}$$

Using $\sqrt{1+x} \approx 1 + x/2$ for $x \ll 1$, equations (23) and (25) can be approximated by the following equations in the case of large internuclear separations, taking only the terms up to R^{-6} into account:

$$V_{\pm} = \frac{C_6^g + C_6^u}{2R^6} \pm H\left[1 + \frac{\left(C_6^g - C_6^u\right)^2}{8H^2R^{12}}\right] \approx \frac{C_6^g + C_6^u}{2R^6} \pm H \tag{26}$$

for the states correlating with 1s + 2s and

$$V_{\pm} = \frac{C_6^g}{R^6} \pm H\left[1 + \frac{\left(C_3^g\right)^2}{2H^2R^6}\right] = \frac{C_6^g \pm (C_3^g)^2/2H}{R^6} \pm H, \tag{27}$$

for the states correlating with 1s + 2p.

Hence it follows that, in the case of HD, all potentials have a long-range dependence on R^{-6}, in contrast with H_2 where the potentials correlating with the 1s + 2p limit have an asymptotic behaviour of R^{-3}. This can be physically understood in terms of identical particles.

In H_2 the nuclei are identical and no distinction can be made as to which atom is excited, giving rise to a two-fold degeneracy. A wavefunction may therefore be written as the superposition of atom A in the ground state and atom B in the excited state and *vice versa*:

$$|\Psi\rangle = \alpha|A\rangle|B^*\rangle + \beta|A^*\rangle|B\rangle. \tag{28}$$

This superposition may in turn be expressed in terms of states where the individual atoms are in a superposition of the ground state and the excited state:

$$\alpha|A\rangle|B^*\rangle + \beta|A^*\rangle|B\rangle = \sum_{i=1}^{2}(a_i|A\rangle + b_i|A^*\rangle)(c_i|B\rangle + d_i|B^*\rangle). \tag{29}$$

The coefficients should be chosen such that terms containing $|A\rangle|B\rangle$ or $|A^*\rangle|B^*\rangle$ vanish. Atoms in such a superposition possess permanent dipoles and the interaction between two permanent dipole moments is proportional to R^{-3}. This phenomenon is called resonant dipole–dipole interaction [16].

In HD, however, the two atoms are not identical and there is no two-fold degeneracy; either one or the other atom is excited. The two atoms are therefore in distinctive states and no superposition can be formed that would result in a dipole. The interaction is in this case dipole-induced dipole and is therefore proportional to R^{-6}.

Finally, we note that in the present section potentials are derived that give a better discription of the HD molecule than the BO potentials and the potentials of the usual adiabatic approximations. Indeed, mixing between different BO-potentials, the ones of opposite g/u symmetry, is invoked and this is by definition, as given at the end of section 1.1, a non-adiabatic coupling.

3.1. *Assignment of the potential curves*

The long-range interactions between hydrogen atoms have been calculated by Stephens and Dalgarno [15], yielding the constants C_n^g and C_n^u that were used as variables in the analysis above. The constants provided by Stephens and Dalgarno are published in atomic units and the potential energy is given by

$$V(R)(\text{au}) = \sum_{n=1}^{\infty} \frac{C_n(\text{au})}{R^n(\text{au})}. \tag{30}$$

For a hydrogen atom with infinite nuclear mass, the atomic units are hartrees for energy ($E_h = 219474.63\ \text{cm}^{-1}$) and the Bohr radius for length ($a_0 = 0.529\,177\,208$ Å) and the units of C_n are thus $[C_n] = \text{au} = E_h\, a_0^n$. If the finite masses of the nuclei are considered, an appropriate scaling of the atomic units has to be incorporated. The energy scales with the reduced mass, while the length is proportional to the reciprocal of the reduced mass. The conversion from atomic units to units of wavenumbers and Bohr radii of C_n is thus

$$\begin{aligned} C_n[\text{cm}^{-1} a_0^n] &= C_n(\text{au}) E_h \left(\frac{\mu}{m_\text{e}}\right)\left(\frac{m_\text{e}}{\mu}\right)^n \\ &= C_n(\text{au}) E_h \left(\frac{m_\text{e}}{\mu}\right)^{n-1}. \end{aligned} \tag{31}$$

The C_n describe the potential shape of two interacting atoms, but the conversion is given in terms of the reduced mass of only one atom. This gives rise to a problem in the case of heteronuclear isotopomers with two atoms of different reduced mass. In the case of HD we used the reduced mass of a non-existing atom, such that two of these atoms would form a molecule with the same reduced mass of the nuclei as in HD. Thus,

$$\frac{1}{\mu_\text{HD}} = \frac{1}{m_\text{e}} + \frac{1}{2}\left(\frac{1}{M_\text{H}} + \frac{1}{M_\text{D}}\right), \tag{32}$$

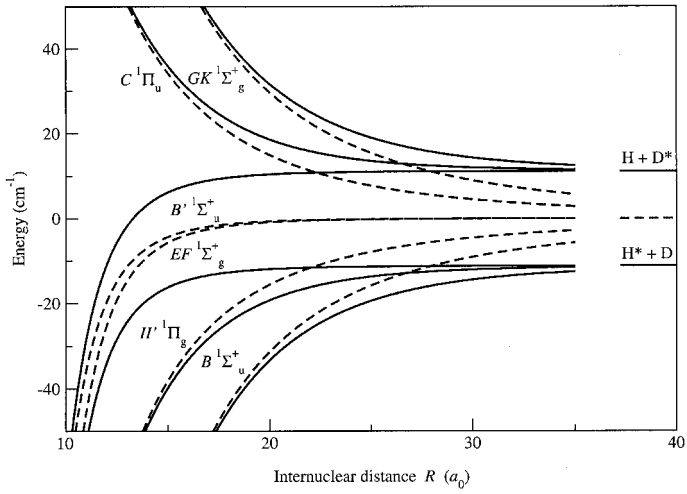

Figure 6. The long-range adiabatic (broken curves) and the constructed potential (full curves) curves are depicted. Both sets of curves are based on the C_n values as calculated by Stephens and Dalgarno [15], although adapted to the case of HD. In homonuclear isotopomers, the adiabatic framework is accurate up to a very high level. In heteronuclear isotopomers, however, this representation breaks down and these potential curves cannot be used at large internuclear distances. As can be seen, the adiabatic curves are still valid for the small internuclear distances. At larger internuclear distances the constructed potentials start to deviate from the adiabatic ones and converge always with R^{-6} to one of the limits. It must be noted that in these curves the long-range interaction terms up to R^{-8} are taken into account. In the absence of spin–orbit interaction, the triplet states have at long range exactly the same R dependence and, hence the same curves apply to the triplet states (with appropriate interchange of g and u labels). The curves of the $GK\,^1\Sigma_g^+$, $C\,^1\Pi_u$, $B'\,^1\Sigma_u^+$, $EF\,^1\Sigma_g^+$, $II'\,^1\Pi_g$ and the $B\,^1\Sigma_u^+$ states resemble the curves of the $f\,^3\Sigma_u^+$, $i\,^3\Pi_g$, $h\,^3\Sigma_g^+$, $e\,^3\Sigma_u^+$, $c\,^3\Pi_u$ and $a\,^3\Sigma_g^+$ states respectively.

with m_e the mass of an electron and M_H and M_D the masses of the nucleus of H and D respectively.

By incorporating these values for C_n (see [8] for the values) and following the procedure as outlined above in section 3, six potentials are found, all doubly degenerate. Twelve electronic states correlate with the $n = 2$ limit of which six are triplet states. In view of the very small spin–orbit interaction in hydrogen the potential energy curves for the triplet states at long range coincide with those of the singlets. Only at binding energies well below 1 cm^{-1} will the difference become significant. In figure 6 the six resulting potentials are plotted and it can be seen how the newly constructed potentials converge to one of the actual limits in HD, rather than the adiabatic limit.

The adiabatic approximation is valid to a high degree in the case of the homonuclear isotopomers. Therefore, with the aid of spectroscopic data the adiabatic curves could be assigned. At long range the singlet potential with the highest energy belongs to the $GK\,^1\Sigma_g^+$ state. The other five singlet states are in order of high to low energy, $C\,^1\Pi_u$, $B'\,^1\Sigma_u^+$, $EF\,^1\Sigma_g^+$, $II'\,^1\Pi_g$ and $B\,^1\Sigma_u^+$. To account for the g–u symmetry breaking, the potentials are evaluated pairwise and this resulted in new potential curves where the upper one was shifted upwards and the lower one downwards with respect to the adiabatic curves. The newly constructed potential

curves converge from the adiabatic curves to the dissociation limits, without crossing each other, as can be seen in figure 6. Therefore, the assignment of these curves follows the same order as in the adiabatic case. The g/u labels, which lose meaning in the asymptotic limit, have been retained in the figure to indicate how the long-range potentials connect to the known potentials at shorter range, where g/u is approximately a good quantum number. In the case of the triplet states, a similar reasoning results in the assignment of the curves. These assignments are given in the figure caption of figure 6.

The pairwise g–u interaction is between GK $^1\Sigma_g^+$ and B $^1\Sigma_u^+$ for $(1s+2p\sigma)$ and between C $^1\Pi_u$ and II$'$ $^1\Pi_g$ for $(1s+2p\pi)$. The interaction results in an asymptotic behaviour proportional to R^{-6}, unlike the proportionality of R^{-3} in the homonuclear isotopomers. The B$'$ $^1\Sigma_u^+$ and EF $^1\Sigma_g^+$ states correlate with $1s+2s\sigma$ and converge asymptotically as R^{-6}, even in the homonuclear species. In HD the pairwise g–u interaction causes the GK, C and B' states to approach the upper limit $H+D^*$, whereas EF, II$'$ and B converge to the lower H^*+D limit.

3.2. *Observation of energy levels near the* n = 2 *threshold in HD*

Around the $n=2$ limit several levels have been observed in HD. Dabrowski and Herzberg have observed rovibrational levels very close to the dissociation limits for all singlet *ungerade* states [5]. For the B state band origins were determined up to $v=43$, so very close to dissociation threshold, whereas vibrational levels up to $v=15$ were observed for the C state. As for the B' state levels were observed for $v=0$–10. The $v=10$ levels with $J\geq 2$ are above the lower (H^*+D) limit; the $J=4$ level is even above second $(H+D^*)$ limit. A tentative assignment is given for B' $(v=11, J=1)$ at $118\,683.6\,\mathrm{cm}^{-1}$.

Two groups focused on laser excitation near the $n=2$ threshold with transitions originating from g symmetry levels. While the Stoicheff group used single-photon excitation from the X $^1\Sigma_g^+$ ground state, the Eyler group used excitation from EF $^1\Sigma_g^+$ intermediate levels. The dissociation energy in HD was determined by Balakrishnan *et al.* [17] as $36\,405.83(10)\,\mathrm{cm}^{-1}$. This value was later confirmed $(36\,405.88(10)\,\mathrm{cm}^{-1})$ by Eyler and Melikechi [18] in work with somewhat higher resolution. In further studies by the Eyler group it was established that at the higher $(H+D^*)$ limit a peculiar resonance occurs, giving rise to a Beutler interference minimum near threshold, when the H(2s) signal is probed [19]. This prevented an accurate determination of the $(H+D^*)$ upper limit in HD.

For the *gerade* states, levels were positively assigned up to $v=23$ for the EF state, $v=3$ for the GK state and $v=3$ for the I state in [5]. All these levels are well below the $n=2$ dissociation limits, although a number of higher-lying unidentified resonances were reported [5]. Many of those resonances were assigned as EF levels in the range from $v=24$ to $v=34$, based on *ab initio* calculations, in the work of Quadrelli *et al.* [20]. In the work of de Lange *et al.* [8], a rotational progression was tentatively assigned to the $EF, v=37$ state (see figure 7).

3.3. *Analysis of levels in the* $I'\,^1\Pi_g$ *state near threshold*

In particular for the I$'$ $^1\Pi_g$ state a detailed experimental analysis was performed for the energy levels in HD [8], as well as in H_2 and D_2 [21]. In the case of H_2 and D_2 the observed level energies agree very well with the energies from *ab initio* calculations by Dressler and Wolniewicz [22]. These calculations were done in the adiabatic representation, i.e. not considering the coupling between the vibrational

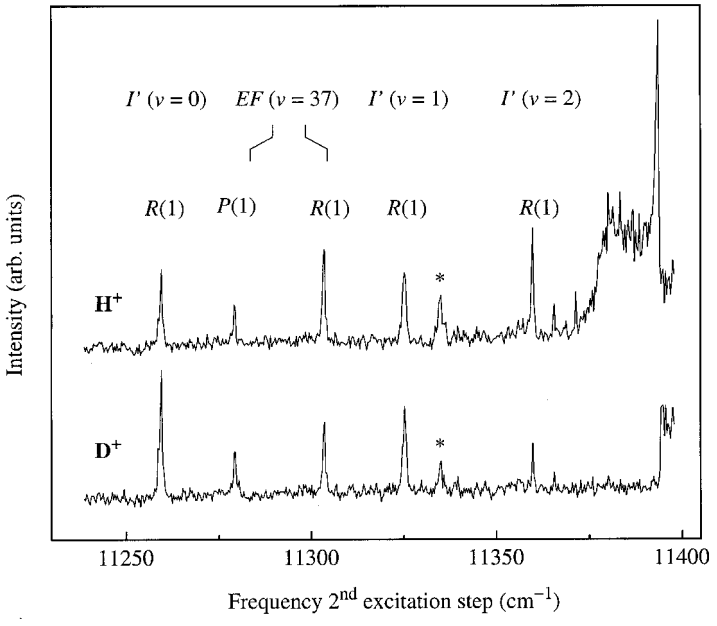

Figure 7. Overview XUV + IR spectrum of HD with the XUV laser tuned on the $B\,^1\Sigma_u^+$–$X\,^1\Sigma_g^+$ $(18,0)$ $R(0)$ transition. The traces show respectively the H^+ and D^+ ion signals obtained after the ionization pulse. The lines are saturation broadened. The continuum onset in the upper trace corresponds to the $H^* + D$ dissociation limit, whereas the onset in the second trace corresponds to the $H + D^*$ dissociation limit. The feature superimposed on the continuum signal in the upper trace is due to an unassigned predissociating state. The line marked with an asterisk is unidentified as well.

motion of the nuclei and the motion of the electrons as is described by equation (11). In the case of H_2 and D_2, this term vanishes and the adiabatic picture is a very good approximation, in the absence of vibrational coupling in the same manifold. However, in the case of HD, this term is of considerable value; at the dissociation limit the interaction is $\approx 20\,\mathrm{cm}^{-1}$, which is even a large fraction of the potential depth of the I′ well ($\approx 200\,\mathrm{cm}^{-1}$).

LeRoy and Bernstein [23] and Stwalley [24] have shown that the binding energies ϵ_v of the upper vibrational levels v in a potential well with asymptotic behaviour C_n/R^n are determined by the following formula:

$$v_D - v \approx a_n \epsilon_v^{(n-2)/2n}, \tag{33}$$

with a_n a constant proportional to C_n and v_D the 'effective' vibrational quantum number at the dissociation limit. This formula, when applied to the adiabatic I′ potential as calculated by Dressler and Wolniewicz [22], reproduces the experimental data in the cases of H_2 and D_2, even for the lowest vibrational levels. Beyond the observed levels, more levels, closer to the dissociation limit, were predicted; in total the I′ outer well should sustain seven and 11 vibrational levels for respectively H_2 and D_2. Applying equation (33) to the same adiabatic potential for HD results in nine vibrational levels. This adiabatic potential converges towards the non-existing adiabatic dissociation limit, i.e. halfway between the two actual limits: $H^* + D$ and $H + D^*$. The energy levels $v \geq 3$ lie all above the lower $H^* + D$ dissociation limit. In

the calculations by Dressler and Wolniewicz [22], one level was even predicted above this limit. Moreover, the asymptotic behaviour follows an R^{-6} dependence in HD in contrast to the R^{-3} dependence in the homonuclear isotopomers, as explained above.

Applying equation (33) to the constructed potential has to be done with caution; the potential changes from an R^{-3} to an R^{-6} dependence and the potential is well beyond the transition regime and follows almost exactly an R^{-6} function only for $v \geq 2$. This has the result that only one data point ($v = 2$) can be used in the analysis. If, nevertheless, equation (33) is applied to the constructed potential, with $n = 6$ and the appropriate value for a_n, one more level is predicted.

Instead of using the approximate LeRoy–Bernstein–Stwalley long-range model, the energy levels can also be calculated directly from the Schrödinger equation. Using the adiabatic potential of Dressler and Wolniewicz [22] for internuclear distances $R < 12$ au and the constructed potential, obtained by diagonalizing the matrix in equation (21), for $R > 12$ au, the energy levels of the I′ state are calculated with the computer program LEVEL 6.1 of LeRoy [25]. Some slight adaptions to the potentials had to be made to interconnect the two potential curves at $R = 12$ au, as described in [8]. The level energies calculated by Dressler and Wolniewicz [22] deviate $\approx 1\,\mathrm{cm}^{-1}$ from the observed energies, whereas the energies based on the constructed potential differ by only tenths of a wavenumber [8]. This validates the procedure to account for the *gerade–ungerade* symmetry breaking, as described at the beginning of this section. Beyond the observed vibrational levels, indeed one more vibrational level ($v = 3$) is predicted with a binding energy of $1.38\,\mathrm{cm}^{-1}$ (for $J = 1$).

Another phenomenon of *g–u* symmetry breaking is directly visible in the excitation spectrum of the I′ state as presented in figure 7. The spectrum shows excitation to the I′ state after preparing the $\mathrm{B}\,^1\Sigma_u^+$ ($v = 18, J = 1, m_J = 0$) intermediate state. Two different signals were recorded simultaneously: H^+ and D^+ ions that were produced after subsequent excitation of the population in the I′ state to above the dissociation limit of the HD^+ ion; this is accomplished by a UV laser photon. Near dissociation threshold an asymmetry in the H^+/D^+ signal ratio appears because the 2p excitation becomes localized on the H side of the molecule. This localization is an indicator of the breakdown of inversion symmetry in HD. Although the efficiencies for H^+ and D^+ detection are not equal and noise plays a role, the gradual trend towards stronger H^+ signals with increasing v is obvious from figure 7. The levels closer to the limit, in the range where $v = 3$ is expected, are not seen at all in the D^+ spectrum. In figure 7 only $R(1)$ lines are allowed to the I′ state; $P(1)$ probes a $J = 0$ level and these are not supported by a Π state and Q transitions with $m_J = 0 \rightarrow 0$ are dipole forbidden with linearly polarized light, as can easily be seen from the $3j$ symbol

$$\begin{pmatrix} J & 1 & J \\ 0 & 0 & 0 \end{pmatrix} = 0. \tag{34}$$

4. Conclusion

An overview is given of several features in the HD molecule connected to the breakdown of the *gerade–ungerade* inversion symmetry. Transitions which are forbidden in homonuclear isotopomers but to some degree allowed in the heteronuclear counterparts were already known. Recently an example of a much stronger

accidental mixing of *g–u* states was found, ranging over a large span of vibrational levels. Furthermore, we have mapped out how adiabatic long-range potentials can be used to construct a different set of potentials, incorporating *g–u* symmetry breakdown near the dissociation limits.

References

[1] Wick. G. C., 1935, *Atti R. Accad. Naz. Lincei*, **21**, 708.
[2] Herzberg, G., 1950, *Nature*, **16**, 563.
[3] Bunker, P. R., 1973, *J. molec. Spectrosc.*, **46**, 119.
[4] Trefler, M., and Gush, H. P., 1968, *Phys. Rev. Lett.*, **20**, 703.
[5] Dabrowski, I., and Herzberg, G., 1976, *Can. J. Phys.*, **54**, 525.
[6] Hinnen, P. C., Werners, S. E., Hogervorst, W., Stolte, S., and Ubachs, W., 1995, *Phys. Rev.* A, **52**, 4425.
[7] Reinhold, E., Hogervorst, W., and Ubachs, W., 1998, *Chem. Phys. Lett.*, **296**, 411.
[8] de Lange, A., Reinhold, E., Hogervorst, W., and Ubachs, W., 2000, *Can. J. Phys.*, **78**, 567.
[9] Born, M., and Oppenheimer, R., 1927, *Ann. Phys.*, **84**, 457.
[10] Bunker, P. R., 1968, *J. molesc. Spectrosc.*, **28**, 422.
[11] Kołos, W., and Wolniewicz, L., 1963, *Rev. mod. Phys.*, **35**, 473.
[12] Wolniewicz, L., 1998, *J. chem. Phys.*, **109**, 2254.
[13] Reinhold, E., Hogervorst, W., Ubachs, W., and Wolniewicz, L., 1999, *Phys. Rev.* A, **60**, 1258.
[14] Huber, A., Udem, T., Gross, B., Reichert, J., Kourogi, M., Packucki, K., Weitz, M., and Hänsch, T. W., 1998, *Phys. Rev. Lett.*, **80**, 468.
[15] Stephens, T. L., and Dalgarno, A., 1974, *Molec. Phys.*, **28**, 1049.
[16] King, G. W., and van Vleck, J. H., 1939, *Phys. Rev.*, **55**, 1165.
[17] Balakrishnan, A., Vallet, M., and Stoicheff, B. P., 1993, *J. molec. Spectrosc.*, **162**, 168.
[18] Eyler, E. E., and Melikechi, N., 1993, *Phys. Rev.* A, **48**, R18.
[19] Cheng, C. H., Kim, J. T., Eyler, E. E., and Melikechi, N., 1998, *Phys. Rev.* A, **57**, 949.
[20] Quadrelli, P., Dressler, K., and Wolniewicz, L., 1990, *J. chem. Phys.*, **92**, 7461.
[21] Reinhold, E., de Lange, A., Hogervorst, W., and Ubachs, W., 1998, *J. chem. Phys.*, **109**, 9772.
[22] Dressler, K., and Wolniewicz, L., 1984, *Can. J. Phys.*, **62**, 1706.
[23] LeRoy, R. J., and Bernstein, R. B., 1970, *J. chem. Phys.*, **52**, 3869.
[24] Stwalley, W. C., 1970, *Chem. Phys. Lett.*, **6**, 241.
[25] LeRoy, R. J., 1995, University of Waterloo Chemical Physics Research Report CP-555.